Electrical Impedance of Layered Atherosclerotic Plaques on Human Aortas

Cornelis J. Slager, Anton C. Phaff, Catharina E. Essed, Nicolaas Bom, Johan Ch. H. Schuurbiers, and Patrick W. Serruys

Abstract—**Electrical impedance measurements were performed on 13 atherosclerotic human aortic segments at 67 measuring spots in order to determine whether or not on the basis of these data a distinction can be made between atherosclerotic lesions and normal tissue. Stenosis localization and guidance of interventional techniques could be among the applications of an impedance measuring technique implemented on a catheter system.**

The experimental results, obtained with a two-electrode measuring technique, show that the apparent resistivity of an atherosclerotic spot does not necessarily deviate much from the resistivity of normal tissue. This is clarified by histology which shows that the majority of lesions has a surface layer of connective, fibrous tissue having almost similar conducting properties as the normal arterial wall. For gaining a deeper understanding of the way in which the measured data come about, a physical model of an atherosclerotic lesion is presented and confronted with the data. Both experimental data and theoretical considerations lead to the conclusion that only when the superficial fibrous layer is absent or very thin in relation to the size of the measuring electrode, the measured resistivity at a lesion is much higher than at normal spots. This occurs as a consequence of the high ohmic properties of the calcified or lipid deposits in the atherosclerotic lesion.

INTRODUCTION

IN recent years much effort has been put in laser recanalization of obstructed atherosclerotic arteries [1]–[3]. Lately, we proposed an alternative technique for vaporizing atherosclerotic plaque: spark erosion [4]. Both techniques, laser vaporization as well as spark erosion, hardly discriminate between atherosclerotic plaque and normal vessel wall, thus carrying the risk of vessel wall perforation [5], [6]. Therefore, sensing techniques must be developed in order to control that only atherosclerotic tissue is attacked. The most obvious way to tackle the problem is to look for physical properties that distinguish atherosclerotic tissue from normal tissue. In the case of spark erosion it seems natural to look for differences in electrical properties in much the same way as it is natural to look for differences in optical properties in the case of the laser [7]–[11]. This is one of the reasons why we decided to perform a study on the electrical impedance of atherosclerotic human aortic segments. Data on this subject are also needed for a better understanding of spark erosion and other new radiofrequency recanalization [12] and remodeling [13] techniques as well as for developing new intra-arterial impedance measuring methods [14].

METHODS AND MATERIALS

One of the main problems in impedance studies is the choice of electrodes. For our purposes we need an electrode that measures impedance at small spots and that is easily applicable on rather irregular surfaces. As the deposition of atherosclerotic plaque along the endothelial surface does not show a regular characteristic pattern it is not expected that anisotropy of its electrical conductance, if present at all, will be predictive for the type of tissue. For these reasons we considered the use of a four electrode impedance measuring method [15] not mandatory. Thus, for the present study we confined ourselves to the much easier to handle two electrode system. The locality of measurement is achieved by using a small spot electrode (area ≈ 0.1 mm^2) in conjunction with a large plate electrode (area ≈ 4 cm^2). The spot electrode consists of a small cavity in connection to a syringe filled with saline. This cavity contains a wrapped up piece of stainless steel foil (≈ 2 cm^2), which is connected to an electrical lead. The connection with the spot of measurement is established by means of a capillary salt-bridge (Fig. 1). The complete electrode is fixed onto a vertical translation system by means of which it can be positioned against the measuring spot. The main advantages of this construction are firstly, a well-defined, stable metal–electrolyte interface of negligible impedance and secondly, a good and reproducible electrical contact with the measurement spot. The stainless steel plate electrode was glued onto the bottom of a Petri dish and connected to the second electrical lead.

Segments of human aorta (area ≈ 25 cm^2) were obtained at 13 autopsy procedures, stored at 4°C under a saline (0.9%) wetted gaze, and used within 24 h. For measurements, the samples were placed upon the saline wetted plate electrode, thus ensuring a good electrical contact between electrode and sample. Next, applying a slight pressure, the spot-electrode was brought in contact

Fig. 1. Outline of the experimental setup.

Fig. 2. Distribution of the apparent resistivity at 67 measuring spots subdivided on basis of the type of tissue contacting the measuring electrode.
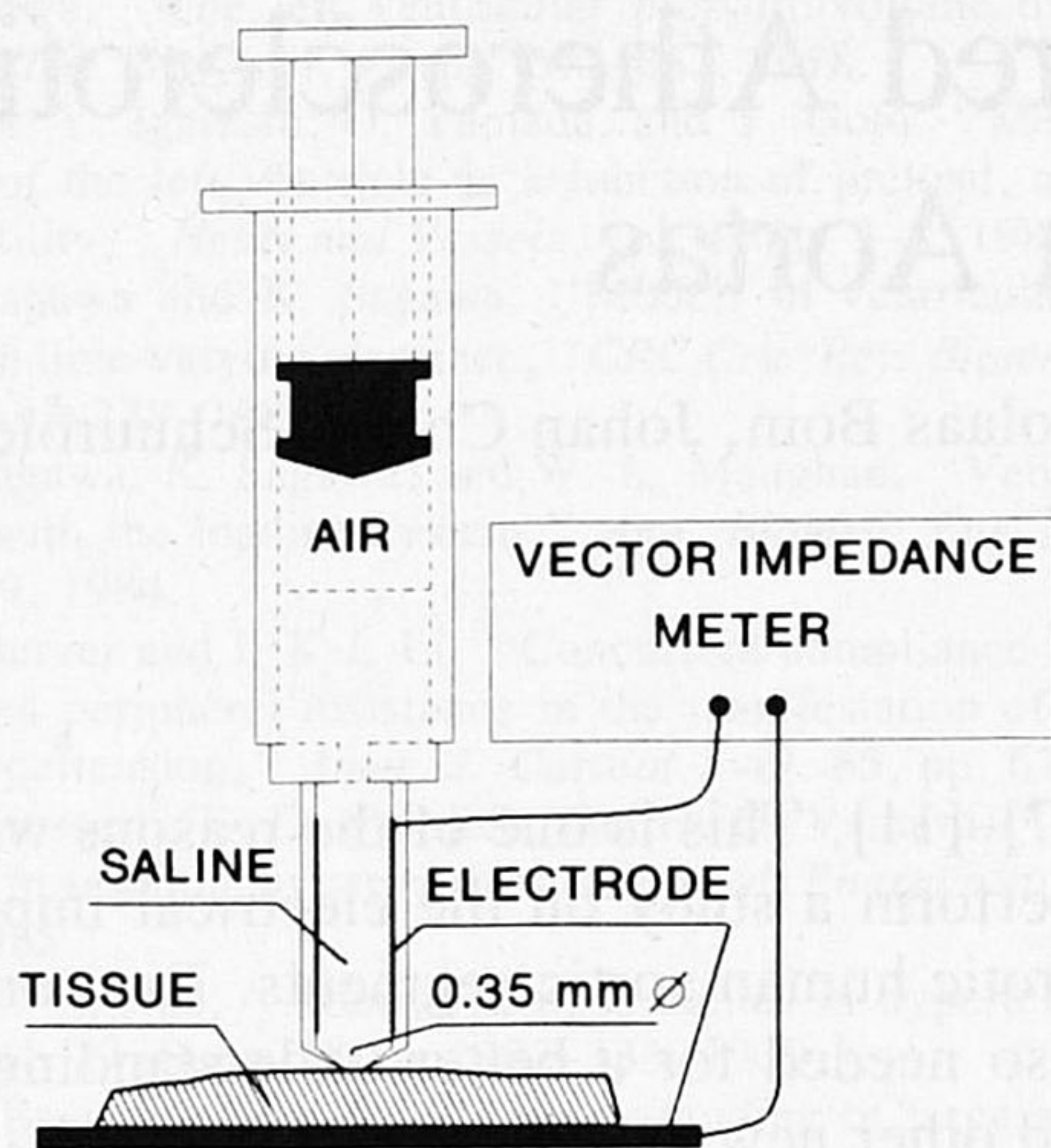
with a well-chosen spot on the top-surface of the sample. Care was taken not to moisten the top-surface of the sample. Saline leakage from the cavity could be prevented by applying an air buffer above the fluid. The impedance between the electrodes was measured by means of an HP 4800A vector impedance meter at frequencies ranging from 5 to 500 kHz and at room temperature (21–23°C). Immediately after the measurement a slight circular impression surrounding the measuring spot could be observed, caused by the electrode's rim. Concentric with this mark a wider circle was drawn by a marking pencil and a map of the aortic segment was sketched to identify and label each measuring spot. For histologic examination strips of tissue were excised from the aortic segments, each containing one measuring spot in the midst. Subsequently, two transverse superficial incisions were made on the strip at equal distance of a few mm from the spot. Thus, the histologic section to be taken through the midst of the strip will show the cross section of the measuring spot just between the two easy identifiable transverse cuts. Staining was performed with hematoxylin-eosin and elastic-van Gieson. The histologic examination was meant to quantify the tissue composition in terms of tissue types and tissue thickness. Part of the measured impedance is caused by the saline path inside the spot-electrode itself. The impedance of the spot-electrode was measured separately by bringing the tip of the electrode in direct contact with the return electrode. At sufficiently high measuring frequencies, the impedance of the metal-electrolyte interface at the plate electrode vanishes [16] and we are left with the ohmic resistance of the salt bridge. Most measurements were carried out with an electrode having a salt bridge resistance of 2.38 kOhm at an electrode aperture of 0.35 mm.

In order to gather an idea about accuracy and reliability of the measuring methods, measurements were done on a saline gel (thickness 5 mm) with known ohmic resistance. For a gel of infinite thickness, the relation between the measured resistance (R), the aperture (d) and the resistivity (ρ) is [17]:
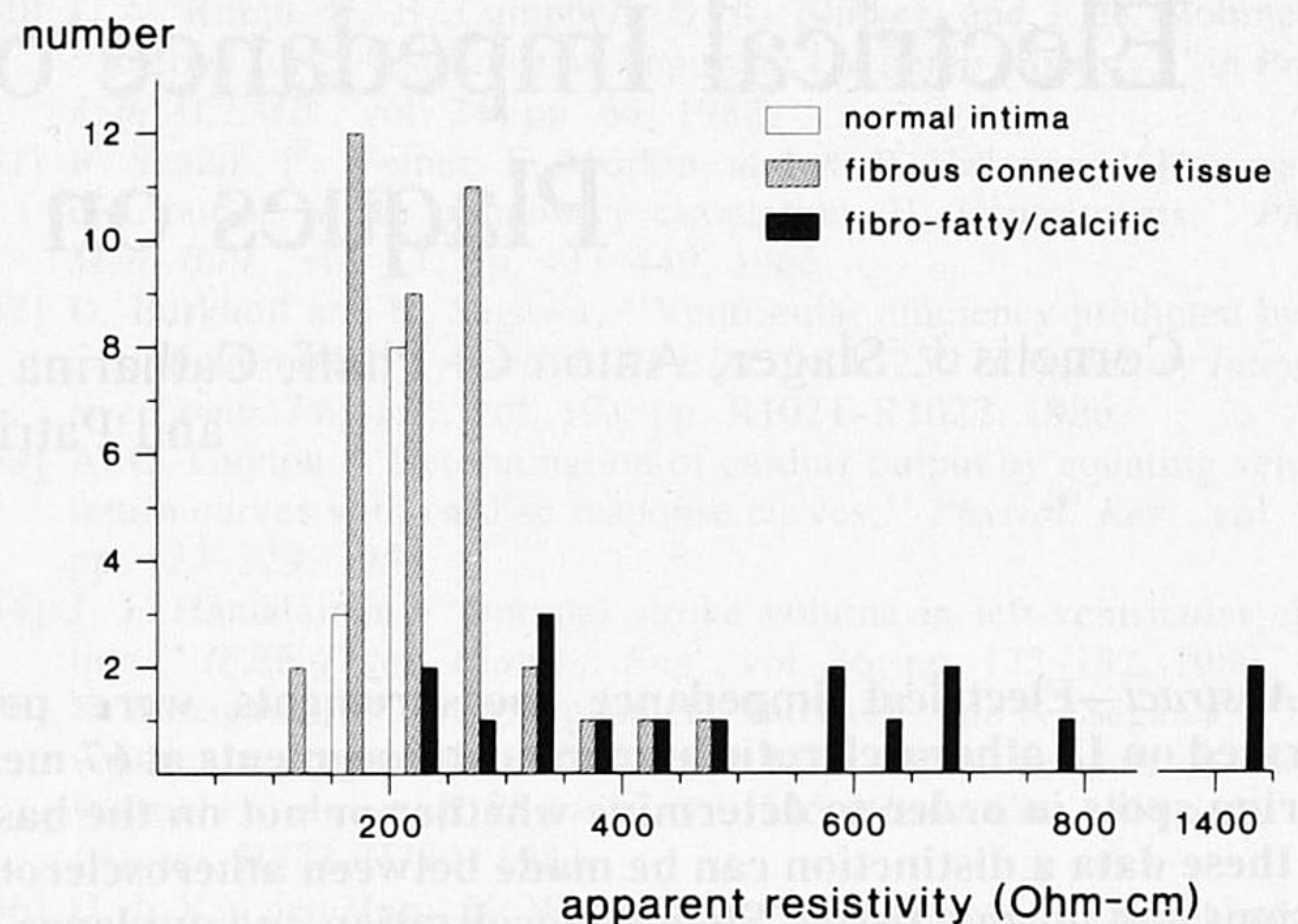
$$\rho = 2d \cdot R \qquad (1)$$

Repeated measurements of the gel resistance by means of the spot-electrode on the same day showed a mean variation of about 2%. As has been observed by microscopy, the aperture of the spot electrode could be deformed slightly over the course of the study. Thus, day-to-day variations could deviate by almost 10%. In order to account for most sources of error in the estimation of the electrode's aperture we performed a calibration procedure on the gel preceding each series of measurements and calculated an apparent aperture d_{app} for each series of tissue impedance measurements, according to:

$$d_{app} = \rho / 2R \qquad (2)$$

where ρ is the known resistivity and R the measured resistance of the gel.

Experimental Results

Impedance was measured at 67 different spots on 13 aortic segments. Each spot was measured a number of times in succession with repeated positioning of the spot electrode. The mean spread in the outcome of the measurements on the same spot did not exceed 5%. As a function of frequency the impedance varied less than 3% and was practically resistive as indicated by the phase angle that never exceeded 4°. After correcting for the salt bridge resistance, the measured resistances ranged from 2 to 30 kOhm.

In practice, it will be convenient to work with an apparent resistivity rather than with the measured resistance. This apparent resistivity ρ_{app} is defined by

$$\rho_{app} = 2d_{app} \cdot R. \qquad (3)$$

For a homogeneous medium of large thickness (i.e., $\gg d_{app}$), ρ_{app} will equal the resistivity of the medium.

TABLE I
EXAMPLE OF DATA OBTAINED FROM ONE AORTIC SEGMENT SHOWING DIFFERENT TYPES OF TISSUE

	Tissue Type and Thickness (mm)			Resistance (Ohm)	Apparent Resistivity (Ohm · cm)	Resistivity of layer 1 (Ohm · cm)
Spot	Layer 1	Layer 2	Layer 3			
A	n 0.21	0	m 1.14	2520	171	169
B	ct 0.67	f 0.84	m 0.80	3450	235	217
C	ct 0.61	f 0.52	m 0.85	3820	260	246
D	ff 0.12	ct 0.16	m 1.27	4850	330	415
E	ff 0.24	ct 0.15	m 1.14	9650	656	820
F	ct 1.33	0	m 0.98	3420	233	240
G	ct 0.82	f 1.17	m 0.97	4190	285	269
H	n 0.20	0	m 1.19	3590	244	265
I	f 0.54	ct 0.23	m 1.14	21120	1436	1626

Abbreviations: ct: fibrous connective tissue, f: fat, ff: fibro-fatty, m: media, n: normal intima.

The group of 67 measuring spots may be divided into three classes consisting of 11 normal spots, 39 atherosclerotic spots characterized by a top layer of fibrous connective tissue, and 17 atherosclerotic spots without such a fibrous cap, showing fatty and calcific components in its superficial layer. The distribution of the apparent resistivity in these classes is shown in Fig. 2. The apparent resistivity of the normal spots is localized between 150 and 250 Ω · cm, whereas the apparent resistivity of the atherosclerotic spots covers a much wider range from 100 Ω · cm up to 1450 Ω · cm. From the histograms it follows that most of the atherosclerotic lesions belonging to the group with a fibrous top layer have an almost normal apparent resistivity.

To gain insight into the results and their interpretation we will discuss a representative example out of the series of 13 aortic segments. On this sample nine well chosen spots were measured. Histologic examination revealed that in most cases the intima was thickened and displayed a layered structure. The histologic findings and the measured values of ρ_{app} are presented in Table I and Fig. 3. For the photograph, hematoxylin-eosin stained sections were selected, which provide the best discrimination between fatty and fibrous tissue components. Only a part (length 2 mm) of the sections covering the measuring spot, has been displayed.

From Table I it is clear that the apparent resistivity of a true atherosclerotic lesion (e.g., B, C) does not necessarily deviate much from the apparent resistivity of a comparatively normal aortic wall (A and H). However, there are also atherosclerotic spots (e.g., D, E) with negligible intima thickening, which have an apparent resistivity that is far greater than the apparent resistivity of a normal spot. The high-resistivity lesions always show fat or calcified deposits being incorporated in the superficial layers, whereas the superficial layer of the low resistivity lesions always consists of pure fibrous connective tissue. This indicates that the apparent resistivity is determined to a high degree by the resistivity of the superficial layer, which is high in case of fat and low in case of connective tissue.
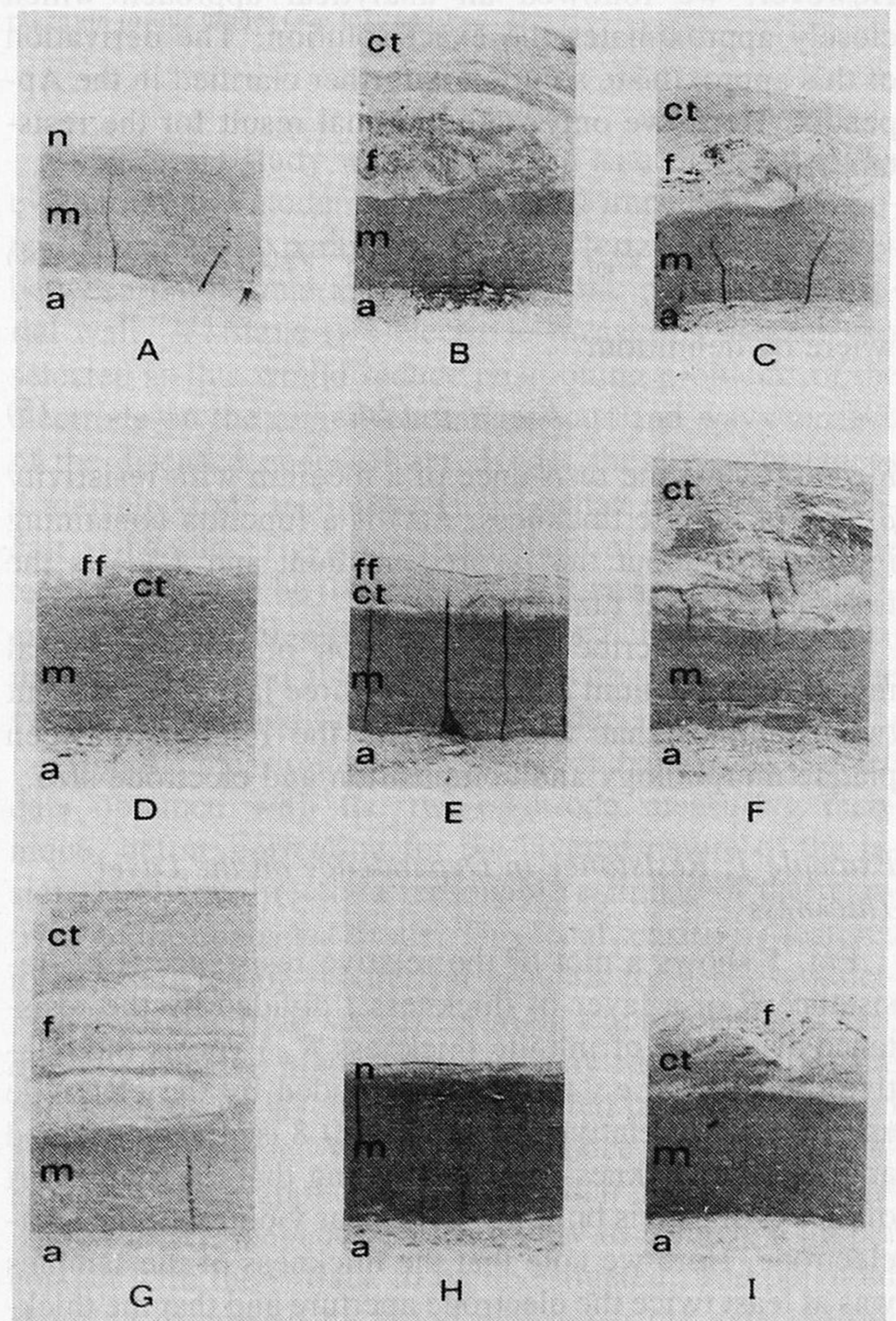

Fig. 3. Histologic sections (displayed length 2 mm) through the aortic wall at nine measuring spots (hematoxylin-eosin stain). Labeling corresponds with Table I. a: adventitia, ct: fibrous connective tissue, f: fat, ff: fibro-fatty, m: media, n: normal intima.

THEORETICAL MODEL

For the purpose of gaining a deeper understanding of the way in which the measured results come about, we will describe a physical model of an atherosclerotic lesion contacted by a two electrode measuring system.

Consider a medium consisting of N layers material of different composition and therefore of different resistivity. The superficial layer is brought into contact with a spot-electrode of aperture d, whereas the remaining surface of this layer is bordered by some medium of infinite resistivity. The bottom layer contacts a medium of finite resistivity, which, for our calculations, supposedly extends to infinity. This medium may be considered as the return electrode (Fig. 4). By definition the zero electrical potential is at infinity. Applying a voltage V to the spot-electrode will impress a current I into the compound medium. Our aim is to compute the electrical resistance (i.e., the ratio V/I) of this configuration.

For the most accurate solution of this problem one probably has to resort to the method of finite elements. However, we followed an analytical approach which closely approximates the exact solution. The derivation of this approximate solution is further clarified in the Appendix. Here, we only state the final result for the resistance R:

$$R = R_{inf} \frac{4}{\pi} \int_0^\infty F(x) \frac{\sin x}{x^2} J_1(x) \, dx \qquad (4)$$

where by definition:

$$R_{inf} = \rho_1/2d. \qquad (5)$$

R_{inf} represents the resistance of a medium with resistivity ρ_1 and of infinite thickness. $F(x)$ is a function containing information about the layered medium and $J_1(x)$ is the first order Bessel function.

Next we describe the application of this theoretical model for a medium consisting of three layers, to present two examples that will elucidate the relation between plaque morphology and composition and electrode size.

Example 1: Resistance in Dependence on the Layer Thickness

Fig. 5 shows a plot of the relative resistance (i.e., resistance R of a layer of thickness t divided by the resistance of a layer of infinite thickness R_∞) versus the relative thickness (i.e., thickness t divided by the electrode aperture d). A relative resistance of 0.8 is already reached at a relative thickness of 1, indicating that the major part of the resistance is built up in the near vicinity of the spot-electrode. Here we note that the thickness of the samples was at least twice the electrode aperture and that the thickness (5 mm) of the gel, used for the calibration of the electrode's aperture, amply suffices.

Example 2: Resistance in Dependence on the Resistivity of the Middle Layer

Fig. 6 shows a plot of the relative resistance R/R_∞ (with $R_\infty = \rho_1/2d$) of a medium consisting of three layers, with thicknesses t_1, t_2, and t_3, as a function of the resistivity of the second (middle) layer, assuming that $\rho_1 = \rho_3$. The three curves correspond with different thicknesses of the superficial layer t_1 being $0.25d$, $0.50d$, and
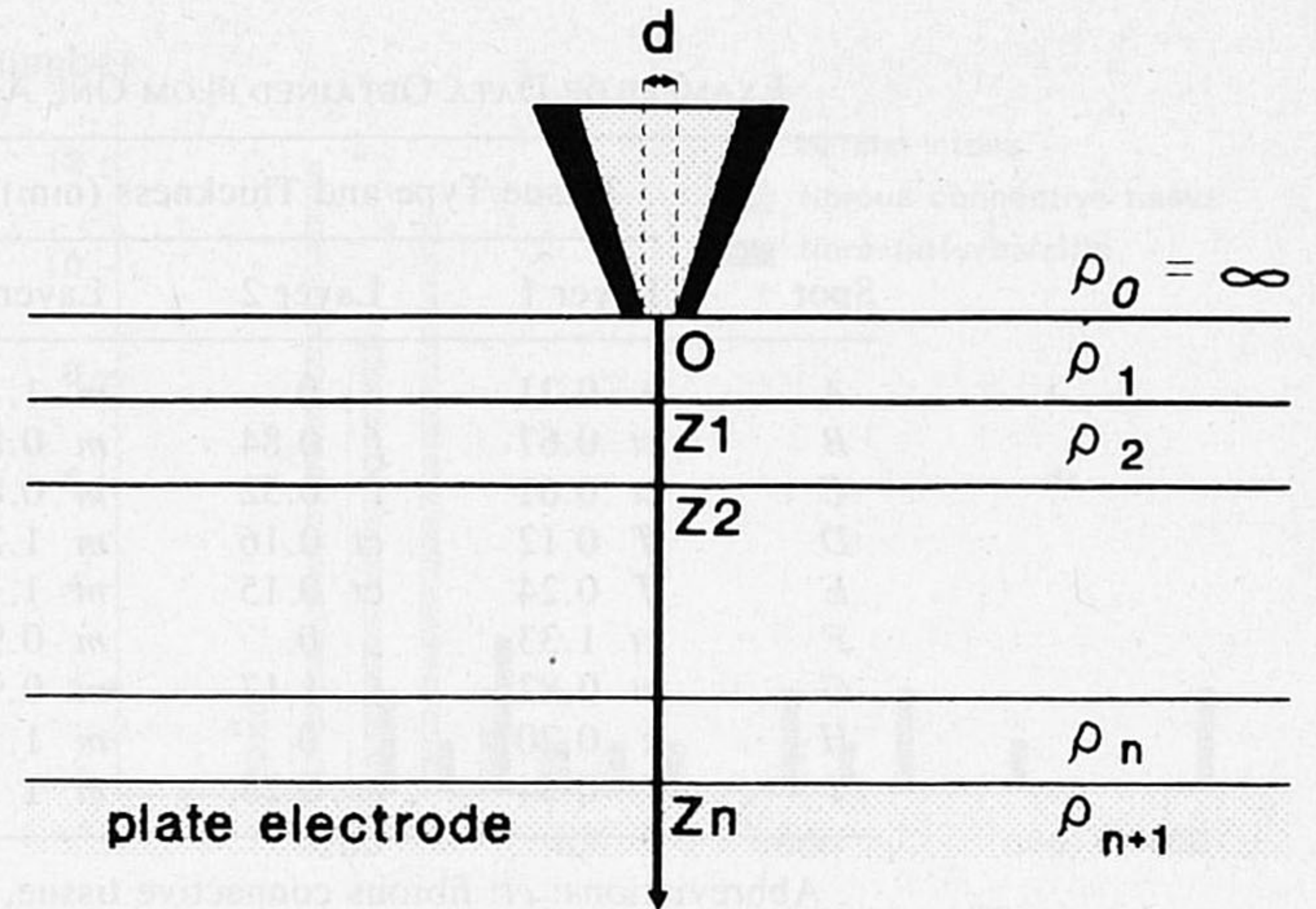

Fig. 4. Physical model of an atherosclerotic lesion between spot-electrode and plate-electrode.
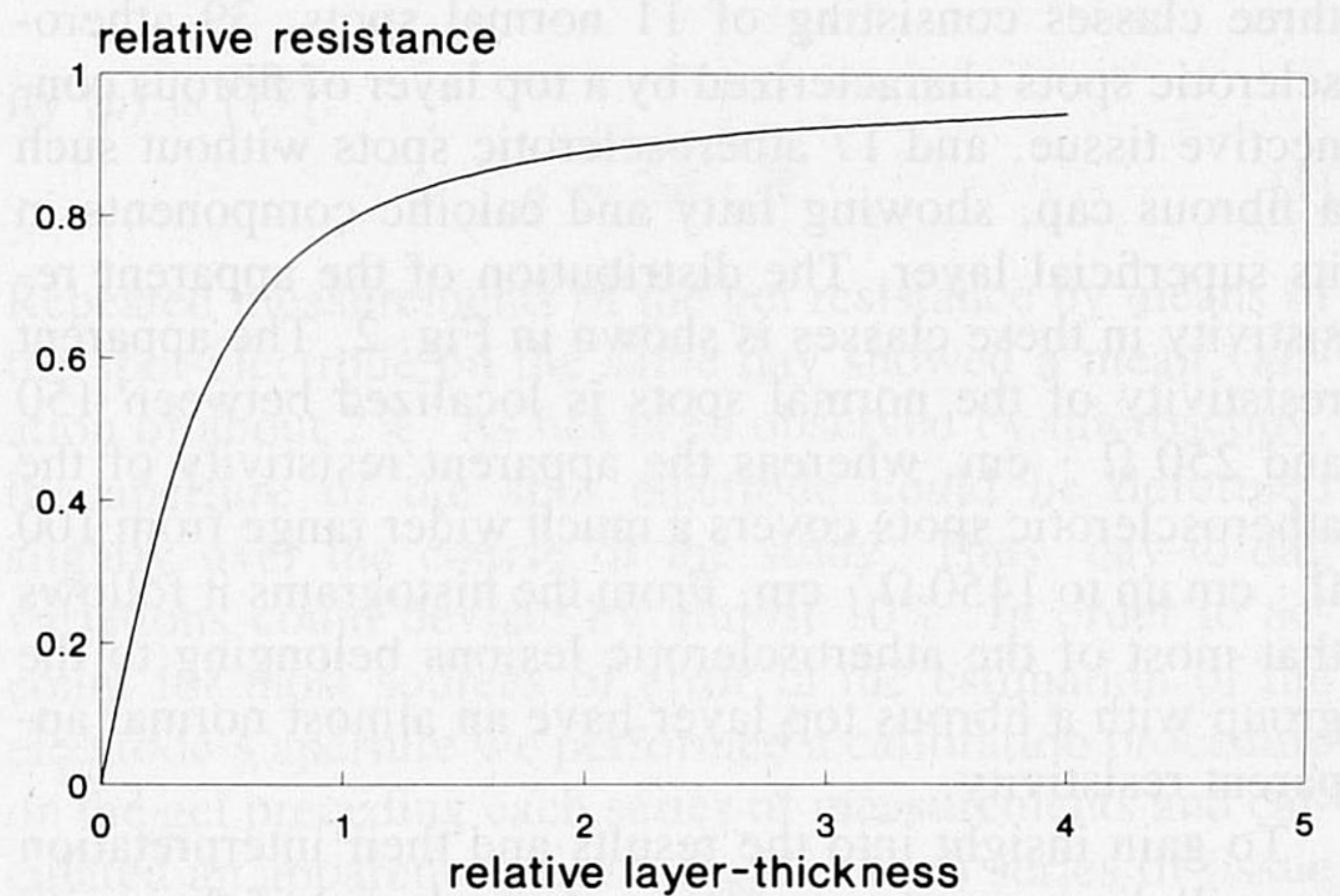

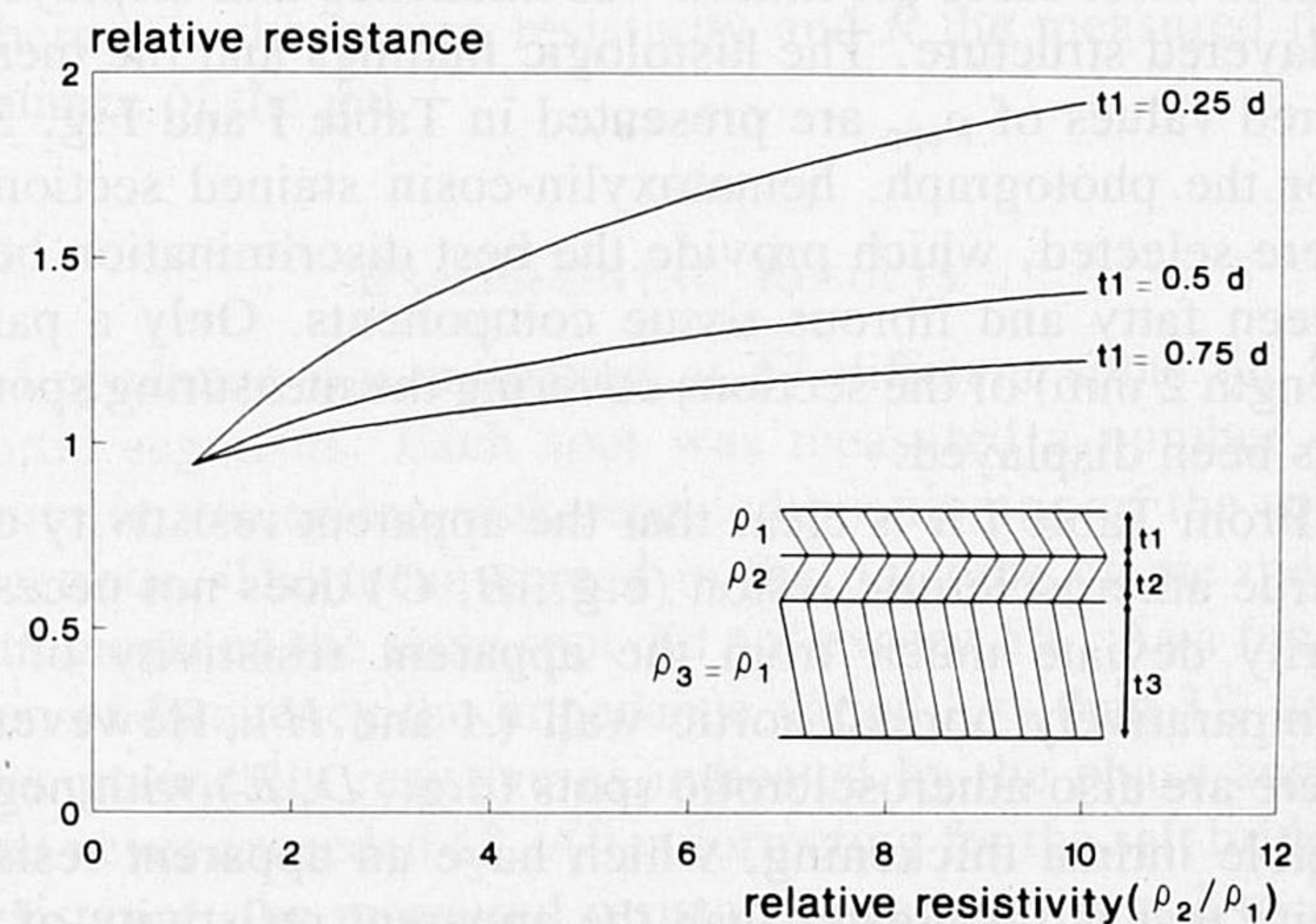Fig. 5. The relative resistance of a homogeneous medium in dependence on the layer thickness/aperture ratio.

Fig. 6. The relative resistance of a layered medium in dependence on the resistivity of the middle layer for three thicknesses (t_1) of the superficial layer related to the electrode aperture d.

$0.75d$ with d being the electrode's aperture. In order to let these curves originate from the same position, the total thickness $t_1 + t_2 + t_3$ is kept at $3.75d$ and $t_2 = 0.75d$. From this figure it is clear that at increasing superficial layer thickness the sensitivity of the resistance to changes

in ρ_2 tends to decrease. It may be stated that for $t_1 \geq 0.75d$ the upper layer quite effectively shields the underlying layers from the spot-electrode.

These two numerical examples evidently show that the measured tissue resistance will be most sensitive to the resistivity of the superficial layer, which is clearly in support of the findings of our measurements.

APPLICATION OF THE MODEL

We analyzed our resistance data in terms of the above described three-layer model in order to see whether the spread in the apparent resistivity can be explained from the way in which the atherosclerotic plaques are composed as layered structures of different tissue types. As no separate impedance data of each type of tissue are available, our way to perform this analysis, is to make a reasonable estimate as to the resistivity of the underlying layers (connective tissue, media) and then to adjust the resistivity of the superficial substance of each measuring spot until the measured and the computed resistances match. For the tissue sample described in Table I the following estimated resistivities of the underlying layer have been applied:

$$\rho_{\text{connective tissue}} = \rho_{\text{media}} = 235 \ \Omega \cdot \text{cm}. \tag{6}$$

Throughout the calculations the impedance of a fourth layer, the adventitia, which contacted the saline wetted return plate electrode (4 cm^2), has been neglected. The estimated contribution of this layer (thickness < 0.5 mm), to the measured resistance is less than 1%. Assuming (6), it necessarily follows from the resistance at spot I that ρ_{fat} = 1626 $\Omega \cdot$ cm. This value for ρ has been used for the enclosed fatty layers in spots B, C and G. In the last column of Table I, the resistivity values of the superficial tissue layer are tabulated as obtained by the above described method. Apparently the resistivity values of the superficial fibro-fatty layers (D, E) change most while the mean resistivity value for connective tissue (A, B, C, F, G, H) equals 234 $\Omega \cdot$ cm which affirms our first estimation. The presence of fat under the intimal connective tissue layer has only a minor influence on the apparent resistivity as can be derived from the data at spots B, C, and G. As suggested by Fig. 2 the apparent resistivity of fibrous tissue covering plaques is somewhat higher than the apparent resistivity of the normal intima. However, when comparing the true resistivities of both types of tissue the outcome may be different. To allow such a comparison to be made in a quantitative way we applied the model on the data of those sites depicted in Fig. 2 which are characterized by either a normal intima or a superficial layer of fibrous connective tissue. The following assumptions were used: the resistivity of fat is 1600 $\Omega \cdot$ cm and the resistivity of the media is equal to the resistivity of the top layer. The results of this approach are depicted in Fig. 7. The similarity of the resistivities of both groups of tissue has increased as a result of this operation. However, as already suggested by the curves shown in Figs. 5 and 6, the effect of this operation is small.
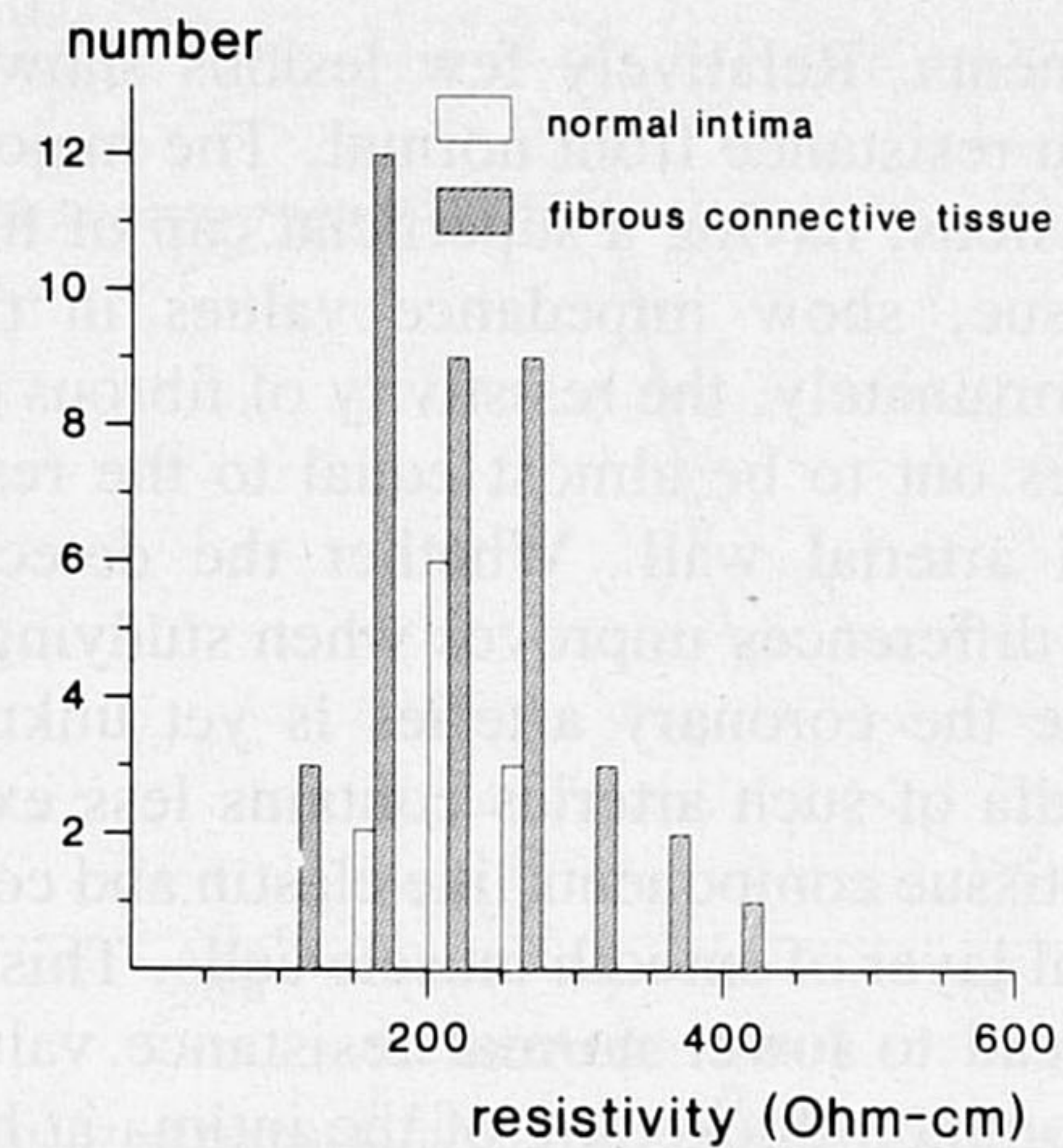

Fig. 7. Distribution of the resistivity of the superficial tissue layer at eleven normal spots and at 39 spots showing fibrous connective tissue, after application of our model (see text and Fig. 2).

DISCUSSION

The present study was undertaken as a first step in the evaluation and modeling of electrical impedance as a potential diagnostic parameter to characterize the differences between the normal and atherosclerotic parts of the arterial wall. A simple two-electrode measuring system was selected as this would reduce positioning problems of the electrode on the rather inhomogeneous and wavy surface of the diseased endothelium. Under these circumstances a four-electrode technique [15] seemed to us more difficult to handle. The major advantage of a four-electrode technique would be the inherent elimination of the impedance of the metal–electrolyte interface. However, a similar function could also be obtained with the two-electrode system, by the addition of a salt bridge.

From the measurement results it can be learned that the data obtained with the two-electrode measuring technique, before correcting for the layered nature of the lesions, provide directly a reasonable estimate of the resistivity of the contacted tissue. This local sensitivity feature, to be predicted on theoretical grounds for a nonsymmetrical two electrode set up, is highly appreciated. Thus, directly decisive impedance data may be obtained of the contacted tissue layer being considered for removal by an ablation technique. Whether impedance measuring techniques will be applicable for vascular tissue characterization in vivo depends on the ability to achieve a proper contact with the surface to be investigated. The potential shunting of current by blood will lower the detectability of differences in tissue impedance. Substitution of blood by low-conducting fluid would reduce this problem but has practical drawbacks. Obviously, the measurement of blood resistivity itself will be the easiest to perform, while the presented model and data of the vascular resistivities will be useful to give an indication of the expected accuracy of this application under varying circumstances [14]. The overlap in impedance of diseased and normal arterial wall must be minimal to provide a useful basis for guidance of intravascular tissue removal techniques. For practical reasons the current investigation was restricted to

aortic segments. Relatively few lesions showed a clear deviation in resistance from normal. The majority of obstructive lesions, having a superficial cap of fibrous connective tissue, show impedance values in the normal range. Unfortunately, the resistivity of fibrous connective tissue turnes out to be almost equal to the resistivity of the normal arterial wall. Whether the detectability of impedance differences improves when studying muscular arteries like the coronary arteries is yet unknown. The normal media of such arteries contains less extracellular connective tissue components like elastin and collagen and a substantial layer of smooth muscle cells. This could theoretically lead to lower normal resistance values. However, the common thickening of the intima at higher age, by fibrous connective tissue addition, may well be sufficient to neutralize this potential advantage. Notable differences between morphology and composition of aortic and coronary plaque are unknown to us. Only the impression exists that ulcerating plaques, missing a fibrous cap, are more frequently seen in the larger elastic arteries than in the smaller muscular type of arteries.

Application of the presented model appeared to be very useful to get a quantitative insight in the parameters determining the sensitivity of the measurement in dependence on the resistivity of the different tissue layers. It also allowed to make a reasonable estimation of the specific resistivity of the contacted tissue layers, Since to our knowledge no data have been published before on the resistivity of atherosclerotic plaques we could not compare most of our findings with data obtained by others. Fat tissue is reported [18] to have a resistivity in the range of 1100–5000 Ω · cm. Except for one superficial true fatty lesion with a resistivity over 1600 Ω · cm falling within this range (Table I) and one calcified lesion with an apparent resistivity over 1400 Ω · cm the remaining 15 lesions without a fibrous cap (Fig. 2) had lower apparent resistivities ranging from 200 to 800 Ω · cm. The tissue composition of the latter group showed a mixture of fibrous and fatty parts which explains its resistivity varying between the value of fibrous connective tissue and that of the true fatty lesion. A tissue type coming close to fibrous connective tissue may be human skin tissue. The resistivity of human skin tissue measured at room temperature and at a frequency of 1 MHz is reported to be 289 Ω · cm [18]. An estimate of the specific resistance of vein, pulmonary artery and bronchus is reported to vary from 250 to 700 Ω · cm [19]. These data compare well with our findings depicted in Fig. 7.

We conclude that our model is very helpful in understanding the characteristics of impedance measurements on layered tissue structures. Generally, the impedance of the layer contacting the measuring electrode will dominate the measured impedance. Constituting atherosclerotic plaque components like fatty and calcified tissues appear to have a much higher resistivity than normal arterial wall. However, in most cases these components are covered by fibrous tissue with a resistivity not much deviating from normal. Therefore it appears to us that only a limited number of lesions may be recognized by *in vivo* applicable impedance measuring methods.

APPENDIX

Derivation of equations describing the resistance of layered atherosclerotic plaques measured by a two-electrode technique using an analytical approach.

As suggested by the symmetry of our problem, we use cylindrical coordinates (r, φ, z) to describe our problem (see Fig. 4). The potential distribution $\varphi_i(r, z)$ in each layer has to obey Laplace's equation:

$$\varphi_i(r, z) = 0 \quad \text{for } i = 1,2, \cdots, N + 1. \quad \text{(A1)}$$

At the interfaces the potential must be continuous and so must be the normal component of the current-density

$$\varphi_i(r, z) = \varphi_{i+1}(r, z) \quad \text{for } z = z_1, \cdots, z_N \quad \text{(A2)}$$

$$\sigma_i \frac{\delta\varphi_i(r, z)}{\delta_z} = \sigma_{i+1} \frac{\delta\varphi_{i+1}(r, z)}{\delta z}$$

$$\text{for } z = z_i, i = 1, \cdots, N$$

$$\text{where } \sigma_i = 1/\rho_i. \quad \text{(A3)}$$

Through the surface of the top-layer no current can pass except at the electrode which is maintained at the potential V

$$\varphi_1(r, z) = V \quad \text{for } 0 \leq r < a \text{ and } z = 0 \quad \text{(A4)}$$

$$\frac{\delta\varphi_1(r, z)}{\delta z} = 0 \quad \text{for } a \leq r < \infty \text{ and } z = 0 \quad \text{(A5)}$$

where a = the radius of the electrode, $2a = d$. Furthermore, the potentials φ_i must vanish at infinity. Thus, everywhere on a closed surface, partly at infinity, either the potential or its normal derivative is specified and therefore a unique, stable solution exists inside this surface.

The solution of (A1) yields [20]–[22].

$$\varphi_i(r, z) = \int_0^\infty \{A_i(k)e^{-kz} + B_i(k)e^{kz}\}J_0(kr)\,dk \quad \text{(A6)}$$

where J_0 is the Bessel function of zero order and where the coefficients $A_i(k)$ and $B_i(k)$ have to be determined from the boundary conditions.

The mixed boundary conditions lead to a pair of dual integral equations, for which, to our knowledge, no analytical solution is available. Therefore, in order to proceed with our analysis, we have to resort to some method of approximation. This can be done by replacing the boundary condition (A4), which prescribes the potential at the electrode by a boundary condition which prescribes the current density at the electrode according to

$$\sigma_1 \frac{\delta\varphi_1(r, z)}{\delta z}\bigg]_{z=0} = \frac{I}{2\pi a}\frac{1}{\sqrt{a^2 - r^2}} \quad \text{for } 0 \leq r < a. \quad \text{(A7)}$$

This is the current density that would exist in case of a homogeneous medium extending to infinity. The validation of the replacement of boundary condition (A4) by boundary condition (A7) will be discussed later on. Again the new boundary equations result in a pair of dual integral equations:

$$\int_0^\infty \{A_1(k) - B_1(k)\} J_0(kr) k \, dk = 0$$

$$\text{for } a \le r < \infty \tag{A8}$$

$$\sigma_1 \int_0^\infty \{A_1(k) - B_1(k)\} J_0(kr) k \, dk = \frac{I}{2\pi a} \frac{1}{\sqrt{a^2 - r^2}}$$

$$\text{for } 0 \le r < a. \tag{A9}$$

The solution to these equations is well known [20]–[22] and reads

$$A_1(k) - B_1(k) = \frac{I}{2\pi\sigma_1} \frac{\sin ka}{ka}. \tag{A10}$$

In order to fulfil the boundary conditions at infinity it is necessary that $B_{N+1} = 0$. Now the interface conditions together with the boundary conditions provide us with $2N + 1$ inhomogeneous equations for the $2N + 1$ unknowns $A_1, B_1, A_2, \cdots A_N, B_2, \cdots B_N$ and A_{N+1}. These equations are solved by straightforward computation using Cramer's rule.

The potential at the surface $z = 0$ is given by

$$\varphi_1(r, 0) = \int_0^\infty \{A_1(k) + B_1(k)\} J_0(kr) \, dk. \tag{A11}$$

As a consequence of the replacement of boundary condition (A4) by boundary condition (A7), this potential does not have a constant value throughout the electrode.

In order to be able to define a unique resistance we must average this potential over the surface of the electrode

$$\langle V \rangle = \frac{1}{\pi a^2} \int_0^a 2\pi r \varphi_1(r, 0) \, dr. \tag{A12}$$

The resistance R is now obtained as $R = \langle V \rangle / I$, which may be written

$$R = \frac{1}{4a} \frac{4}{\pi} \int_0^\infty F(x) \frac{\sin x}{x^2} J_1(x) \, dx$$

$$\text{with } F(x) \text{ defined by} \tag{A13}$$

$$F(x) = \frac{A_1(x/a) + B_1(x/a)}{A_1(x/a) - B_1(x/a)}. \tag{A14}$$

All information about thickness and resistivity of the layers is contained in this function. We will write down $F(x)$ explicitly for $N = 3$

$$F(x) = \frac{\beta(\delta + h)(\epsilon + \beta nm) + \delta(\delta h + 1)(\epsilon m + \beta n)}{\beta(\delta - h)(\epsilon + \beta nm) + \delta(\delta h - 1)(\epsilon m + \beta n)}$$

$$\tag{A15}$$

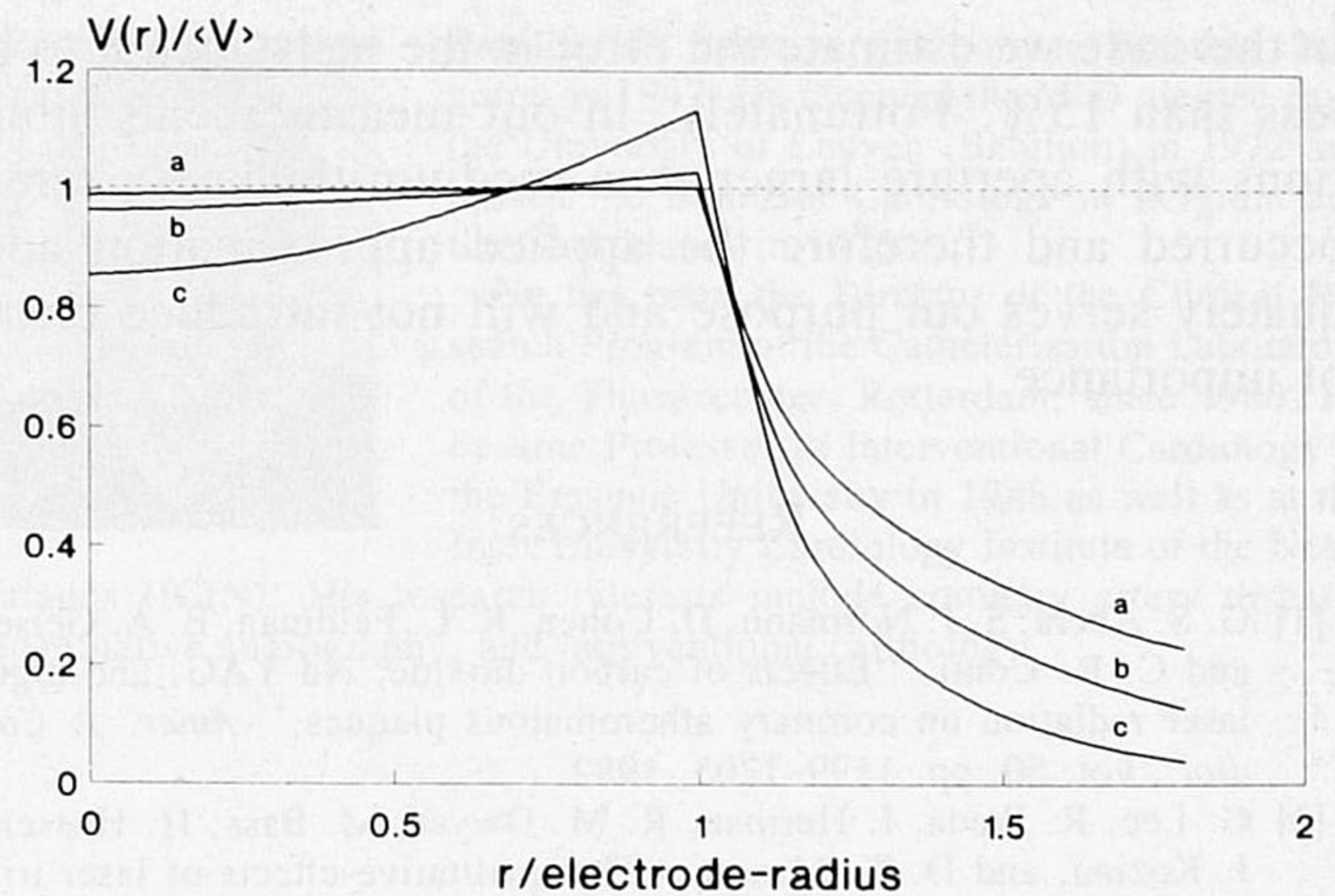

Fig. 8. Normalized potential profile over the electrode and over the surface of the top layer as obtained by our model. The curves a, b, and c correspond to different ratios of aperture/layer thickness being 1, 2, and 4, respectively.

where the following definitions hold

$$h = \frac{\sigma_1 - \sigma_2}{\sigma_1 + \sigma_2} \qquad \delta = \exp(2xz_1/a)$$

$$m = \frac{\sigma_2 - \sigma_3}{\sigma_2 + \sigma_3} \qquad \beta = \exp(2xz_2/a)$$

$$n = \frac{\sigma_3 - \sigma_4}{\sigma_3 + \sigma_4} \qquad \epsilon = \exp(2xz_3/a).$$

If $\sigma_1 = \sigma_2 = \sigma_3 = \sigma_4$ then $h = m = n = 0$ and it follows that $F(x) = 1$. Inserting $F(x) = 1$ in formula (A13) one obtains for the resistance $R = \rho_1/2d$, that is Maxwell's classical result is restored.

Our ultimate aim is the evaluation of the right-hand side of expression (A13). This can be done numerically, making use of NAG-library routines for quadrature as well as the first order Bessel function.

Here it is worthwhile to note that, after our computations, we became aware of the fact that our problem carries much similarity with a problem from geophysics as reported already in 1930 by Stefanesco et al. [23]. They solved part of the present problem (i.e., the potential distribution over the top-surface) for an electrode with aperture $d = 0$, that is a point-electrode. The validation of the replacement of boundary condition (A4) by boundary condition (A7) will now be discussed. The most obvious way to do this, is to look how the potential at the electrode behaves under the impression of the current distribution as described by condition (A7). For several layer-thicknesses the potential profile; i.e., $V(r)$ as a function of r has been computed using formula A11. In order to obtain a normalized result, each potential profile was divided by the appropriate mean voltage $\langle V \rangle$. The results are depicted in Fig. 8 for three different layer-thicknesses, being d, $0.5d$, and $0.25d$, with d being the electrode's aperture. The deviation of $V(r)$ from $\langle V \rangle$ may serve as a measure of the reliability of our method of computing resistances. Even at an aperture of four times the layer-thickness the potential does not deviate more from $\langle V \rangle$ than 15%. So

in this case we estimate the error in the resistance R to be less than 15%. Fortunately, in our measurements situations with aperture larger than medium-thickness rarely occurred and therefore the applied approximation adequately serves our purpose and will not introduce errors of importance.

REFERENCES

[1] G. S. Abela, S. J. Normann, D. Cohen, R. L. Feldman, E. A. Geiser, and C. R. Conti. "Effects of carbon dioxide, Nd-YAG, and argon laser radiation on coronary atheromatous plaques," *Amer. J. Cardiol.*, vol. 50, pp. 1199-1205, 1982.

[2] G. Lee, R. Ikeda, I. Herman, R. M. Dwyer, M. Bass, H. Hussein, J. Kozina, and D. T. Mason, "The qualitative effects of laser irradiation on human arterio-sclerotic disease," *Amer. Heart J.*, vol. 105, pp. 885-889, 1983.

[3] J. M. Isner, R. F. Donaldson, L. I. Deckelbaum, R. H . Clarke, S. M. Laliberte, A. A. Ucci, D. N. Salem, and M. A. Konstam, "The excimer laser: Gross, light, microscopic and ultrastructural analysis of potential advantages for use in laser therapy of cardiovascular disease," *J. Amer. Coll. Cardiol.*, vol. 6, pp. 1102-1109, 1985.

[4] C. J. Slager, C. E. Essed, J. C. H. Schuurbiers, N. Bom, P. W. Serruys, and G. T. Meester, "Vaporization of atherosclerotic plaques by spark erosion," *J. Amer. Coll. Cardiol*, vol. 5, pp. 1382-1386, 1985.

[5] G. Lee, R. M. Ikeda, M. C. Chan, M. H. Lee, J. L. Rink, R. L. Reis, J. H. Theis, R. Low, W. J. Bommer, A. H. Kung, E. S. Hanna, and D. T. Mason, "Limitations, risks and complications of laser recanalization: A cautious approach warranted," *Amer. J. Cardiol.*, vol. 56, pp. 181-185, 1985.

[6] J. M. Isner and R. H. Clarke, "Laser angioplasty: Unravelling the Gordian knot," *J. Amer. Coll. Cardiol.*, vol. 7, pp. 705-708, 1986.

[7] M. R. Price, T. F. Deutsch, M. M. Matthews-Roth, R. Margolis, J. A. Parrish, and A. R. Oseroff, "Preferential light absorption in atheromas *in vitro*," *J. Clin. Invest.*, vol. 78, pp. 295-301, 1986.

[8] M. J. C. van Gemert, R. Verdaasdonk, E. G. Stassen, G. A. C. M. Schets, G. H. M. Gijsbers, and J. J. Bonnier, "Optical properties of human blood vessel wall and plaque," *Lasers Surg. Med.*, vol. 5, pp. 235-237, 1985.

[9] P. M. Selzer, D. Murphy-Chutorian, R. Ginsburg, and L. Wexler, "Optimizing strategies for laser angioplasty," *Invest. Radiol.*, vol. 20, pp. 860-866, 1985.

[10] C. Kittrell, R. L. Willet, C. de los Santos-Pacheo, N. B. Ratliff, J. R. Kramer, E. G. Malk, and M. S. Feld, "Diagnosis of fibrous arterial atherosclerosis using fluorescence," *Appl. Opt.*, vol. 24, pp. 2280-2281, 1985.

[11] G. S. Abela, J. M. Seeger, E. Barbieri, D. Franzini, A. Fenech, C. J. Pepine, and C. R. Conti, "Laser angioplasty with angioscopic guidance in humans," *J. Amer. Coll. Cardiol.*, vol. 8, pp. 184-192, 1986.

[12] V. Hombach, M. Höher, G. Arnold, P. Osypka, M. Kochs, T. Eggeling, H. W. Höpp, H. Hirche, and H. H. Hilger, "Die Hochfrequenzangioplastie eine neue Methode zur Rekanalisation verschlossener arterieller Gefässe," *Corvas*, vol. 2, pp. 67-73, 1987.

[13] G. J. Becker, B. I. Lee, B. F. Waller, K. J. Barry, J. Kaplan, R. Connolly, R. G. Dreesen, and P. Nardella, "Radiofrequency balloon angioplasty. Rationale and proof of principle," *Invest. Rad.*, vol. 23, pp. 810-817, 1988.

[14] L. W. Martin, R. Zawodny, and R. A. Vogel, "Impedance measurement of absolute arterial diameter using a standard angioplasty catheter," *J. Amer. Coll. Cardiol.*, vol. 11, p. 130A, 1988.

[15] S. Rush, J. A. Abildskov, and R. McFee, "Resistivity of body tissues at low frequencies," *Circ. Res.*, vol. 12, pp. 40-50, 1963.

[16] B. Onaral, H. H. Sun, and H. P. Schwan, "Electrical properties of bioelectrodes," *IEEE Trans. Biomed. Eng.*, vol. 31, pp. 827-832, 1984.

[17] J. C. Maxwell, *A Treatise on Electricity and Magnetism*. 3rd ed. Dover, reprint 1954.

[18] L. A. Geddes and L. E. Baker, "The specific resistance of biological material: A compendium of data for the biomedical engineer and physiologist," *Med. Biol. Eng.*, vol. 5, pp. 271-293, 1967.

[19] H. P. Schwan and C. F. Kay, "Specific resistance of body tissues," *Circ. Res.*, vol. 4, pp. 664-670, 1956.

[20] J. D. Jackson, *Classical Electrodynamics*. New York, Wiley 1962, Ch. 3, p. 54.

[21] I. N. Sneddon, *Mixed Boundary Value Problems in Potential Theory*. Amsterdam: North-Holland, 1966, ch. 4, p. 80.

[22] W. R. Smythe, *Static and Dynamic Electricity*. New York: McGraw-Hill, 1968, ch. 5, p. 121.

[23] S. Stefanesco, C. Schlumberger, and M. Schlumberger, "Sur la distribution électrique potentielle autour d'une prise de terre ponctuelle dans un terrain à couches horizontales, homogènes et isotropes," *J. Physique*, vol. 1, pp. 132-140, 1930.
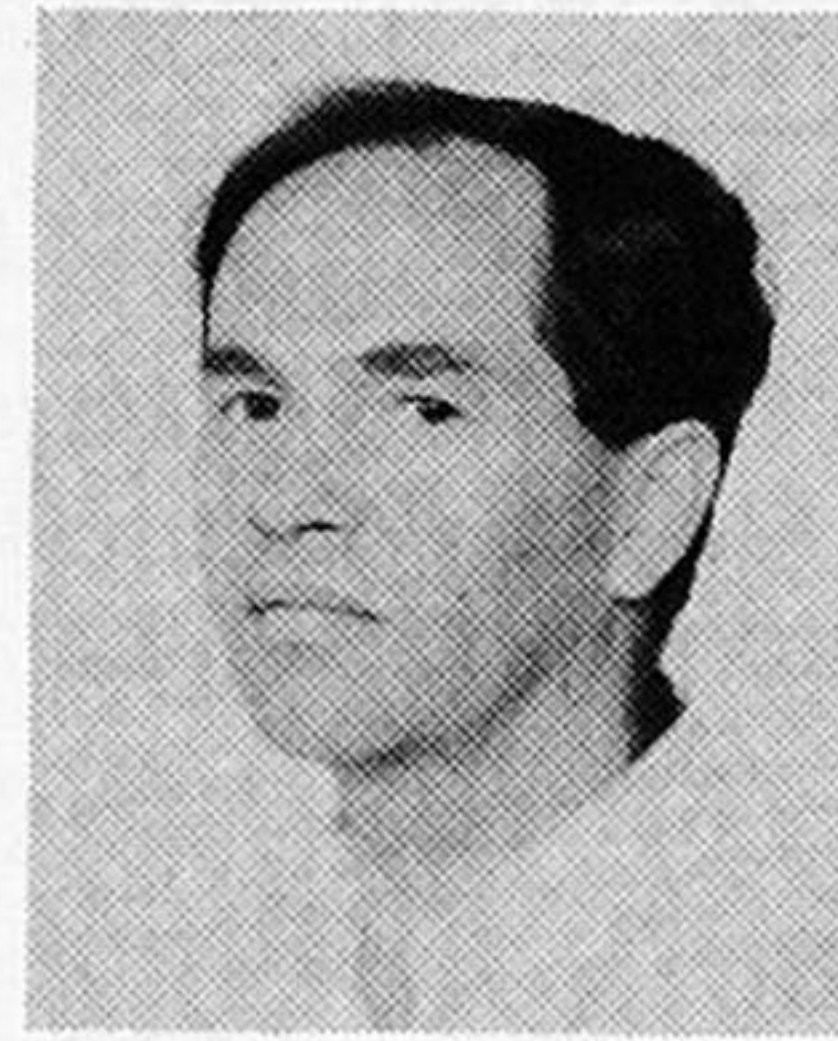
Cornelis J. Slager was born in Scherpenisse, Zeeland, The Netherlands, in 1945. He received the M.Sc. degree in electrical engineering from Delft University of Technology in 1971. During his graduate work he invented an automated border recognition system for ventriculograms.

After teaching electronics at the Delft University, he joined the Biomedical Technology Group of the Thoraxcenter, University Hospital Dijkzigt-Rotterdam in 1973. His research interests are in quantitative processing of cardiological images and in diagnostic and therapeutic instruments for interventional cardiology.

Anton C. Phaff was born in Amsterdam, The Netherlands, in 1952. He received the M.Sc. degree (summa cum laude) in solid state physics from the Free University of Amsterdam in 1979 and the Ph.D. degree in physics from the Eindhoven University of Technology. His thesis concerned a subject from the magnetism at low temperatures.

During 1986 and 1987 he joined the Biomedical Technology department of the Thoraxcenter, Erasmus University Rotterdam. Today he still maintains ties with this group.

Catharina E. Essed was born in Amsterdam, The Netherlands, in 1953. She graduated in medicine from the Erasmus University, Rotterdam, in 1978 and specialized in pathology between 1978 and 1983.

During and after her specialization she worked mainly in cardiovascular pathology. Since 1989 she is assigned as a surgical pathologist to the Laboratory for Public Health in Friesland, the Netherlands.
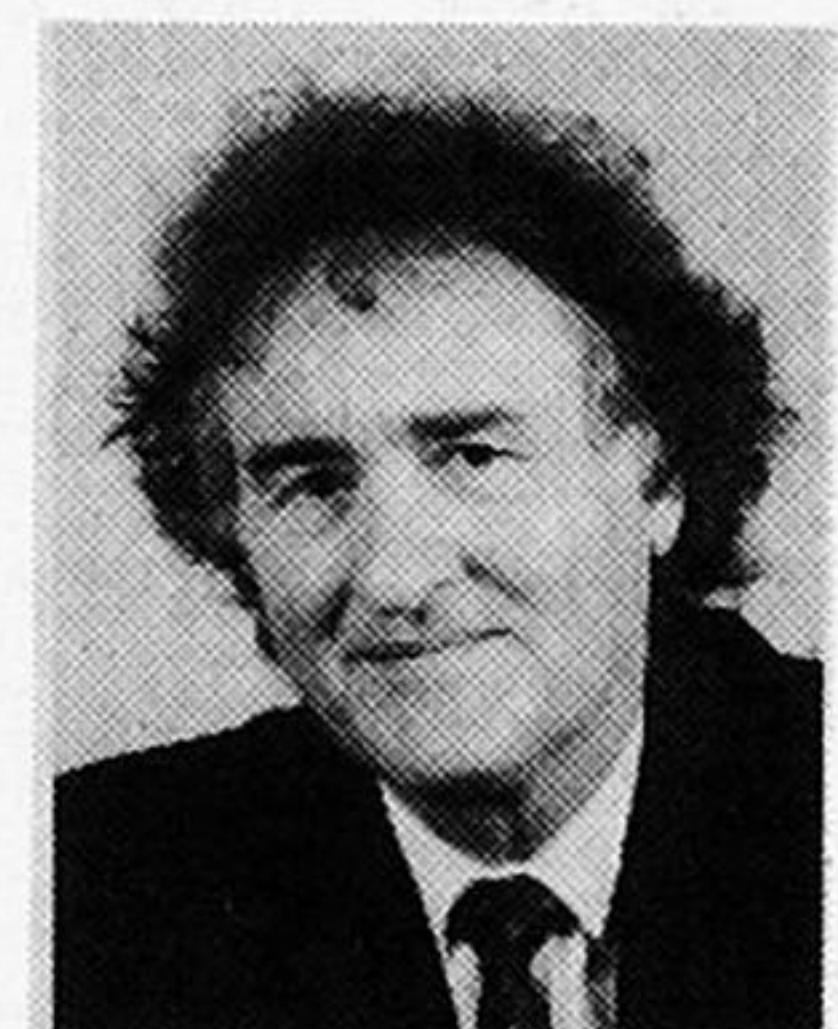
Nicolaas Bom was born at Velsen, The Netherlands, in 1937. He received the M.Sc.EE degree from the University of Technology, Delft, in 1961 and the Ph.D. from the Erasmus University, Rotterdam, in 1972.

In 1969 he joined the Thoraxcenter of the Erasmus University to set up a diagnostic ultrasound research and development program. Since 1974, he has been head of the Biomedical Engineering Group of the Thoraxcenter. He became Professor of Medical Ultrasound at the Interuniversity Cardiology Institute of the Netherlands (ICIN) and at the Erasmus University Rotterdam in 1979. In 1987 he received a honorary doctorate from the Technological faculty of the University of Lund, Sweden, for his work and inventions in the field of echocardiography.

Dr. Bom has been a member of the Scientific Board and the Board of Directors of ICIN since 1983.

Johan Ch. H. Schuurbiers was born in Vlaardingen, The Netherlands, in 1950. He received a degree in electrical engineering from the College of Aeronautics and Electronics, Den Haag in 1972.

Until 1976, while studying electronic engineering, he was involved in industrial engineering. In 1976 he joined the Cardiology Department of the Dijkzigt Hospital as a research technician. His interests are in real-time image processing and analysis techniques, digital/analog hardware, software for biomedical signal processing and data acquisition and technical aspects of interventional cardiology.

Patrick W. Serruys was born in Brussels, Belgium, in 1947. He received the M.D. degree from the University of Leuven (Belgium) in 1972 and passed the Board of Cardiology in Belgium and the Netherlands in 1976.

He has been the Director of the Clinical Research Program of the Catheterization Laboratory of the Thoraxcenter, Rotterdam, since 1980. He became Professor in Interventional Cardiology at the Erasmus University in 1988 as well as at the Inter University Cardiology Institute of the Netherlands (ICIN). His research interests include coronary artery disease, quantitative angiography, and interventional cardiology.